JACS
JOURNAL OF THE AMERICAN CHEMICAL SOCIETY

Communication

pubs.acs.org/JACS

Ultrastrong Alkali-Resisting Lanthanide-Zeolites Assembled by [Ln_{60}] Nanocages

Jie Dong,[†] Ping Cui,[†] Peng-Fei Shi, Peng Cheng, and Bin Zhao*

Department of Chemistry, Key Laboratory of Advanced Energy Material Chemistry, MOE, and Collaborative Innovation Center of Chemical Science and Engineering (Tianjin), Nankai University, Tianjin 300071, China

Supporting Information

ABSTRACT: Zeolites, as one of the most important porous materials, are most widely utilized in sorbents, catalysis, and ion-exchange fields. However, the multifunctional lanthanide-zeolites constructed exclusively by lanthanide ions and oxygen linkers are to our knowledge unknown hitherto. Herein, we, for the first time, report the unique structure and multifunctions of lanthanide zeolites (**1·Gd**, **1·Tb**, **1·Dy**), featuring 60 nuclear [Ln_{60}] nanocages as building blocks and ultrastrong alkali-resisting. These compounds possess extremely high stability and still retain single crystallinity after treatment in boiling water, 0.1 M HCl, and 20 M NaOH aqueous solutions. Magnetic studies revealed **1·Gd** has large magnetocaloric effect with $-\Delta S_m^{max}$ = 66.5 J kg^{-1} K^{-1}, falling among the largest values known to date. Importantly, these lanthanide-zeolites themselves can efficiently catalyze the cycloaddition of CO_2 with epoxides under mild conditions. Our finding extends the conventional zeolites to lanthanide counterparts, opening a new space for seeking novel and/or multifunctional zeolites.

Zeolites, as one of the most important porous materials, have been attracting significant attention from both academia and industry, due to the fundamental curiosity in diverse structures and their wide applications in industry for catalysis, adsorption/separation, drug delivery, sensing, etc.[1−3] A lot of efforts have been made to the design and construction of porous materials with zeolite-type topology, and many outstanding contributions have prompted the great progress of this field. It is well-known, that zeolites are constructed from the building units, in most cases, limited to Si and/or Al (T) tetrahedrons connected by oxygen (O) linkers[4] and many other zeolite-like inorganic materials such as the aluminophosphates and transition metal phosphates have also been discovered.[5] Furthermore, the modification of zeolites through replacing those T-sites with other heteroatoms, for example, iron,[6a] titanium,[6b] gallium,[6c] and boron,[6d] etc., leads to the unique structures and versatile applications. Inorganic−organic hybrid zeolite-type materials have recently also been developed as represented by zeolite-like metal−organic frameworks (ZMOFs).[7] Most of the existing zeolite frameworks, especially Si- and Al-based zeolites, can easily decompose or collapse in strong alkali environments, thus greatly restricting their practical applications. Therefore, it is necessary and crucial from both industry applications and fundamental research perspectives to seek novel zeolite frameworks with strong alkali-resistance. It has been documented that more than 210 unique zeolite frameworks have been identified since the first zeolite was artificially synthesized under hydrothermal conditions by Barrer's group[8] in 1940s. Besides, a large number of lanthanide hybrids materials based on zeolite were constructed and show wide applications in optical and catalytic fields.[9] Nonetheless, to our knowledge, the multi-functional lanthanide-zeolites constructed exclusively by lanthanide ions and oxygen linkers have not yet been reported prior to our work herein.

Compared with existing zeolite materials, lanthanide-zeolites are anticipated to possess the following advantages: (1) the unique inner $4f^n$ electron configuration of lanthanide ions will endow various functions to such type of zeolites, such as luminescence, magnetic property, diverse catalytic activity, and bioimaging contrast agents, which have been presented in lanthanide oxide/hydroxide compounds;[10,11] (2) lanthanide-zeolites would exhibit high thermal stability and strong alkali-resistance because of high coordination number and the hard Lewis acid character of lanthanide ions; (3) more importantly, the successful construction of lanthanide-zeolites would open a new space in zeolite field, even such zeolites can further hybridize with the conventional zeolites to generate new porous materials. However, the synthesis of lanthanide zeolites remains a big challenge because the single lanthanide ion hardly serves as four-connected T centers in typical zeolite structures.

Herein, we for the first time report the synthesis, structure, and multifunctions of three lanthanide-zeolite networks: $\{[Ln_3(\mu_6\text{-}CO_3)(\mu_3\text{-}OH)_6]OH\}_n$ (Ln = Gd (**1·Gd**); Tb (**1·Tb**); Dy (**1·Dy**)). All of them possess *SOD* zeolite topology (Figures 1 and S1) and are assembled by [Ln_{60}] nanocages, in which 60 lanthanide ions are bridged by OH^- anions. Such lanthanide-hydroxide zeolite structure features excellent stability in boiling water, 0.1 M HCl and even 20 M NaOH aqueous solutions, and under these conditions the molecular structures still can be clearly analyzed by crystallography, demonstrating their ultrastrong alkali tolerance. The magnetic cooling and catalytic activity in fixing CO_2 reactions were also systematically investigated. These findings provide new insights for the design and synthesis of novel zeolite materials.

Crystallographic analyses revealed that they are essential isomorphous, which can also be confirmed by powder X-ray diffraction (PXRD, Figure S2). Thus, the structure of **1·Gd** was selected as a representative example to describe. The structure of **1·Gd** features an unprecedented 3D *SOD*-topology network

Received: September 23, 2015
Published: December 11, 2015

DOI: 10.1021/jacs.5b10000
J. Am. Chem. Soc. 2015, 137, 15988−15991

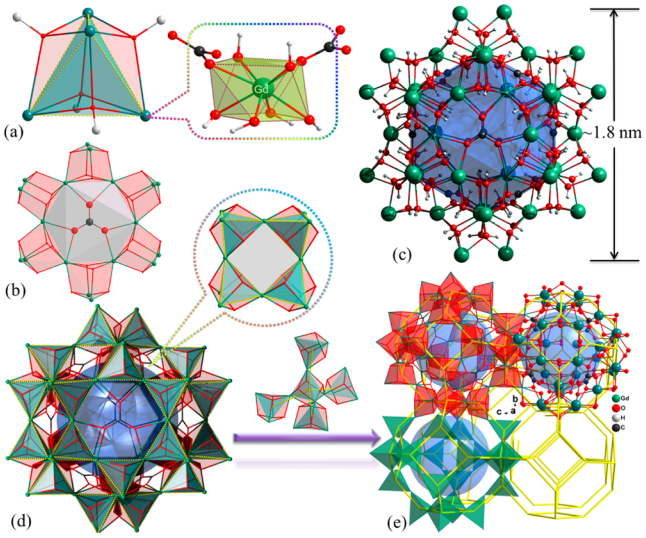

Figure 1. (a) Cubane-like building block $[Gd_4(OH)_4]$. (b) μ_6-CO_3^{2-} ion centered at the face of six-cubane wheel. Ball–stick (c) and stick (d) models of the $[Gd_{60}]$ nanocage built from 24 $[Gd_4(OH)_4]$ cubanes. (e) Three-dimensional framework with *SOD* topology assembled by $[Gd_{60}]$ nanocage. Blue spheres indicate the cavity inside the cages.

built from $[Gd_{60}]$ nanocages, which consists of 24 $[Gd_4(OH)_4]$ cubane-like clusters (Figure 1). In the cube unit, the eight-coordinated Gd^{3+} and the μ_3-OH^- ions alternately occupy the vertices (Figure 1a). Each gadolinium atom in a square-antiprismatic arrangement is coordinated by eight oxygen atoms from six hydroxide and two carbonate groups. Each $[Gd_4(OH)_4]$ cube is connected to four identical neighbors via sharing mode of gadolinium atom, which is represented as a tetrahedral building block. The μ_6-CO_3^{2-} anions bridge six $[Gd_4(OH)_4]$ cubanes to form a six-cubane wheel (Figure 1b). It should be noted that the CO_3^{2-} anion is generated as a coproduct from decomposition of starting material.[11] Furthermore, 24 vertex-sharing $[Gd_4(OH)_4]$ cubanes are linked together to result in the formation of a nanocage $[Gd_{60}(\mu_3\text{-}OH)_{96}(\mu_6\text{-}CO_3)_8]$ with a size of ~1.8 nm (Figure 1c,d). The nanocage possesses six $[Gd_4(OH)_4]$ windows and a valid cavity of ~10 Å in diameter occupied by counterions OH^- (Section S3, Figures S3 and S4). Interestingly, without any bridges of organic ligands, the $[Gd_{60}]$ nanocage as a building block is assembled into a 3D cationic framework with cage-based channels by sharing corners (Figure 1e). Comparably, the reported Er_{60} cage is a discrete cluster, and the adjacent clusters were effectively separated by ligand L-threonine, failing to generate 3D frameworks.[11] To our knowledge, **1·Gd** is the first cationic lanthanide-zeolite material, showing a *SOD* topology.

For **1·Gd**, **1·Tb**, and **1·Dy**, the high connectivity of lanthanide ions and strong lanthanide-oxygen bonds in cubane-like $[Ln_4(OH)_4]$ unit maybe endow them excellent stability in aqueous solutions with wide pH range. To confirm the idea, the stability of **1·Gd** was first checked. Thus, as-synthesized single crystals of **1·Gd** were immersed in aqueous solutions of NaOH (5, 10, 15, and 20 M) and HCl (0.1 and 1 M) with different time at room temperature, respectively. Crystallographic analyses were carried out to directly determine any structural changes after treatment. For as-synthesized **1·Gd**, it crystallizes in the cubic space group *I*432 with $a = b = c = 12.6563(4)$ Å and $V = 2027.30(12)$ Å^3. After immersion in solutions above-mentioned, no obvious differences in morphology, except in 1 M HCl, color, and transparency can be observed, as well as their unit-cell parameters are also similar to that of **1·Gd** crystallized under solvothermal condition (Tables 1 and S1), which suggests that

Table 1. Crystallographic Data of 1·Gd after Treatments in Moisture and Strong Acidic and Strong Basic Medium

Conditions	as-synthesized **1·Gd**	20M NaOH	0.1M HCl	boiling water
Time	No	3 days	6 hours	3 days
Cryst. syst.	cubic	cubic	cubic	cubic
Space group	*I*432	*I*432	*I*432	*I*432
$a = b = c$ (Å)	12.6563(4)	12.6541(5)	12.6597(5)	12.6596(4)
V (Å^3)	2027.30(12)	2026.25(14)	2028.95(14)	2028.90(11)
R1/*wR2*	0.0387/0.0872	0.0773/0.1467	0.0442/0.1044	0.0473/0.1042
$[Gd_4(OH)_4]$ Cluster				

structures do not change. Moreover, the experimental and simulated PXRD patterns are also well consistent with each other, further indicative of no phase transition or framework collapse even in 20 M NaOH (Figure S5). However, when crystals of **1·Gd** are soaked in 1 M HCl solution, observable change in morphology, color, and transparency will occur in 5 min. The vanishing and very weak intensity of PXRD peaks together with no diffraction data from X-ray crystallography suggest the loss of crystallinity or the decomposition of $[Gd_4(OH)_4]$ cubanes under the interaction with acid. It should be noted that the frameworks of **1·Gd** still retain intact even after treatment with concentrated NaOH (20 M) and 0.1 M HCl, clearly demonstrating the exceptionally high chemical stability of lanthanide-zeolites. Similarly, **1·Tb** and **1·Dy** also show super stability toward 0.1 M HCl and 20 M NaOH solutions (Table S2 and Figure S6). Comparably, zeolitic imidazole frameworks (ZIFs) are normally instable toward strong acidic and strong basic medium, which greatly restricts their practical applications.[12] Thermally, they all display high thermal stability (Figure S7), and no obvious weight loss occurs below 320 °C. Variable temperature PXRD of **1·Gd** demonstrated that phase remains unchanged until 330 °C (Figure S8), further confirming high thermal stability and good crystalline state at elevated temperatures.

Gd^{III} containing clusters are normally excellent candidates as molecule-based magnetic coolers due to large-spin ground state ($^8S_{7/2}$), magnetic isotropy, low-lying excited spin states, and weak superexchange interactions.[13] For **1·Gd**, the $\chi_M T$ value decreases with decreasing temperature (Figure S9), which probably originates from the antiferromagnetic (AF) interaction between adjacent Gd^{3+}. The result of χ_M^{-1} vs T fitted by the Curie–Weiss law with $\theta = -4.37$ K further confirmed this weak AF interaction (Figure S10). For evaluating the magnetocaloric effect (MCE), the magnetization from 2 to 10 K was measured (Figure S11). At 2 K the field-dependent magnetization shows a steady increase with increasing field and reaches complete saturation of 21.16 Nβ under 7 T (cal. 21 Nβ for three Gd^{3+}). According to the Maxwell equation, the magnetic entropy change, $-\Delta S_m(T) = \int[\partial M(T,H)/\partial T]_H \, dH$, can be obtained from the experimental magnetization data at various magnetic fields and temperatures (Figure 2). The $-\Delta S_m$ value shows a gradual increase with increasing ΔH and decreasing temperature ($T \geq 3$ K), giving a maximum of 66.5 J kg^{-1} K^{-1} at 3 K for $\Delta H = 8$ T, which is lower than the expected value of 79.7 J kg^{-1} K^{-1} for three uncoupled

DOI: 10.1021/jacs.5b10000
J. Am. Chem. Soc. 2015, 137, 15988–15991

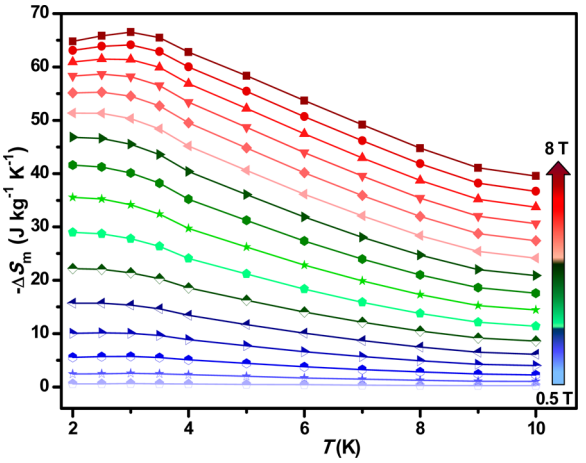

Figure 2. Temperature-dependencies of $-\Delta S_m$ for **1·Gd**.

Gd^{3+} based on $-\Delta S_m = nR\ln(2s+1)$, where R is the gas constant and $s = 7/2$ for Gd^{3+}. The significant divergence between them mainly originates from the AF interactions and crystal-field effects.[14] In all reported molecule magnetic cooling materials, only a few compounds have $-\Delta S_m{}^{max}$ of above 50.0 J kg^{-1} K^{-1}, which are summarized in Table S3, and the largest one is 71.6 J kg^{-1} K^{-1}.[15c] Comparably, at ΔH = 7 T, **1·Gd** possesses the maximum $-\Delta S_m$ of 61.5 J kg^{-1} K^{-1}, which is larger than those of most reported compounds and falls among the largest known values.[15] Surprisingly, the maximum values of $-\Delta S_m$ for **1·Tb** and **1·Dy** are 20.9 J kg^{-1} K^{-1} at 5 K for ΔH = 8 T and 20.2 J kg^{-1} K^{-1} at 6 K for ΔH = 8 T (Figures S12 and S13), respectively. They are much smaller than that of **1·Gd** (66.5 J kg^{-1} K^{-1}), and the large difference among them can be ascribed to significant magnetic anisotropy of Tb^{3+} and Dy^{3+}.

For **1·Tb** and **1·Dy**, although the plots of $\chi_M T$ vs T show similar trend, it is rather difficult to clearly analyze their magnetic interactions due to the orbital contributions.[16] The alternating current (AC) magnetic susceptibilities of **1·Tb** and **1·Dy** were performed to investigate their dynamics of magnetization. The result revealed that the out-of-phase ($\chi_{M''}$) component for **1·Dy** change with the frequency increase, indicating that **1·Dy** possesses single molecular magnet behavior (Figures S14–S16).

Considering the super stability and strong Lewis-acidity of lanthanide-zeolites mentioned above, the catalytic capacity of the lanthanide-zeolite as a catalyst was explored, and here the transformation of CO_2 with epoxides as a model reaction was chosen based on the following considerations: (1) CO_2 is an abundant, nontoxic, renewable, and low-cost C1 source and can potentially serve as a useful building block in synthetic chemistry;[17] (2) as one of the major green-house gases, CO_2 is responsible for the climate change and global warming, and it is necessary to decrease the concentration of CO_2 in atmosphere; and (3) chemical transformation of CO_2 can produce various high value products.[18]

1·Gd, **1·Tb**, and **1·Dy** show similar catalytic activity for cycloaddition of epoxides with CO_2 to afford cyclic carbonates (Table S4). **1·Gd** was used as a representative to examine the scope of the substrates. Under nBu$_4$NBr (TBAB) as an additive and **1·Gd** as a catalyst, both electron-withdrawing and electron-donating terminal epoxides can be converted to the corresponding cyclic carbonates in good yields (Table 2) under mild temperature (60 °C) and pressure (1 atm). The desired product 4-phenyl-1,3-dioxolan-2-one was obtained in 70% yield after 12 h (Table 2, entry 1a). However, under the absence of **1·Gd**, the

Table 2. 1·Gd Catalyzed Cycloaddition Reactions of CO_2 with Epoxides to Cyclic Carbonates

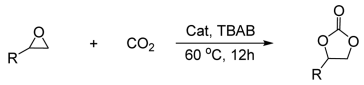

Entry	Catalyst	Subs	Prod	Yield[c]
1a[a]	**1·Gd**			70%
1b[b]	—			23%
2[a]	**1·Gd**		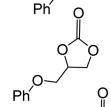	92%
3[a]	**1·Gd**	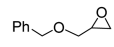	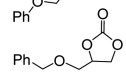	94%
4[a]	**1·Gd**			97%
5[a]	**1·Gd**			38%

[a]Reaction conditions: epoxides (1 mmol), **1·Gd** (16.3 mg, 0.075 mmol gadolinium), and nBu$_4$NBr (2.5 mol %), CO_2 (1 atm gauge pressure). [b]The same conditions as footnote *a* but without the catalyst. [c]Isolated yield.

corresponding product was obtained with very low yield of 23% (Entry 1b), suggesting the **1·Gd** as a catalyst plays an important role in the reaction. The cycloaddition reactions of CO_2 with 1,2-epoxy-3-phenoxypropane (Entry 2) and benzyl glycidyl ether (Entry 3) were effectively catalyzed in higher yields (92% and 94%) than Entry 1a, which can be explained by the electron-withdrawing substituents facilitate nucleophilic attack of the *N*-methylhomopiperazine during the ring opening of the epoxide,[19] as well as different steric hindrance of substituents access to Gd^{3+} catalytic centers (Section S6). When epichlorohydrin (Entry 4) was used, the desired product was generated with excellent yield of 97%. However, the internal epoxide, cyclohexene oxide (Entry 5), is converted to the corresponding cyclic carbonate with low yield of 38%, mainly because of the high steric hindrance.[20]

The nature of the reaction has also been explored. Under same conditions as those in Table 2, entry 1a, after removal of catalyst at 4 h, it was found that the transformation of epoxide dramatically decreases (Section S6, Figure S17). Additionally, inductively coupled plasma (ICP) analysis of the reaction mixture filtrate excluded the possibility of Gd leaching, confirming the heterogeneous nature of the reaction. Note that the catalyst was reused for successive three times without showing any significant drop in catalytic performance of the catalyst (Table S4, Entries 1b–1d), and the robust framework of catalyst **1·Gd** still remains intact after the catalytic reaction, which was confirmed by PXRD investigations (Figure S18). Compared with the common heterogeneous catalysts like zeolites and MOFs (Table S5), **1·Gd** as lanthanide-zeolite exhibited well catalytic activity without loading additional catalysts.

Based on the reported mechanism of the cycloaddition of CO_2 and epoxides,[17a] we propose a tentative reaction mechanism (Figures S19–22). Epoxides are activated by the eight-coordinated Lewis acidic Gd^{3+} sites in **1·Gd** (Figure S21), and the Br^- promotes the ring-opening of the epoxides effectively. Then CO_2 around the window attack C atoms and Br^- is removed to finish the catalytic reaction. Considering the small

DOI: 10.1021/jacs.5b10000
J. Am. Chem. Soc. 2015, 137, 15988–15991

window size, the substrates can not enter the [Gd_{60}] nanocage and react with CO_2. Comparably, Gd_2O_3, $Gd(OH)_3$, and $Gd(NO_3)_3$ did not display significantly catalytic activity (Table S4). The results imply the high density of eight-coordinated Gd^{3+} in [Gd_{60}] nanocage plays a crucial role in promoting the reaction.

In summary, we first constructed the 3D lanthanide-zeolite frameworks assembled by [Ln_{60}] nanocages. The resulting lanthanide-zeolites exhibit exceptional chemical stability toward strong acid and strong base, and even keep single crystal state under 20 M NaOH for 3 days. Magnetic studies illustrated large magnetocaloric effect ($-\Delta S_m^{max} = 66.5$ J kg^{-1} K^{-1}) for **1·Gd** and single molecular magnet-like behavior for **1·Dy**. Interestingly, without loading other catalysts, these lanthanide-zeolites themselves can well catalyze the chemical conversion reactions of CO_2 with various epoxides. This work was hoped to open a new space in pursuing novel and/or multifunctional zeolites. By utilizing of difference of acid-alkalitolerance for lanthanide-zeolites and conventional zeolites, template-guided synthesis of lanthanide zeolites with much bigger porosity is currently under investigation in our group.

■ ASSOCIATED CONTENT

Supporting Information

The Supporting Information is available free of charge on the ACS Publications website at DOI: 10.1021/jacs.5b10000.

Complete experimental details and supplementary figures and tables (PDF)
Characterization of materials (CIF)
Characterization of materials (CIF)

■ AUTHOR INFORMATION

Corresponding Author

*zhaobin@nankai.edu.cn

Author Contributions

†These authors contributed equally to this work.

Notes

The authors declare no competing financial interest.

■ ACKNOWLEDGMENTS

This work was financially supported by the 973 Program (2012CB821702), NSFC (21571107, 21473121, and 21421001), SFC of Tianjin (15JCZDJC37700), 111 project (B12015), and MOE Innovation Team (IRT13022 and IRT13R30) of China.

■ REFERENCES

(1) (a) Davis, M. E. *Nature* **2002**, *417*, 813. (b) Primo, A.; Garcia, H. *Chem. Soc. Rev.* **2014**, *43*, 7548. (c) Feng, P. Y.; Bu, X. H.; Stucky, G. D. *Nature* **1997**, *388*, 735.

(2) (a) Lin, Q. P.; Bu, X. H.; Mao, C. Y.; Zhao, X.; Sasan, K.; Feng, P. Y. *J. Am. Chem. Soc.* **2015**, *137*, 6184. (b) Mintova, S.; Jaber, M.; Valtchev, V. *Chem. Soc. Rev.* **2015**, *44*, 7207. (c) Hudson, M. R.; Queen, W. L.; Mason, J. A.; Fickel, D. W.; Lobo, R. F.; Brown, C. M. *J. Am. Chem. Soc.* **2012**, *134*, 1970.

(3) (a) Huang, L. M.; Wang, Z. B.; Sun, J. Y.; Miao, L.; Li, Q. Z.; Yan, Y. S.; Zhao, D. Y. *J. Am. Chem. Soc.* **2000**, *122*, 3530. (b) Zhou, Y. M.; Zhu, H. G.; Chen, Z. X.; Chen, M. Q.; Xu, Y.; Zhang, H. Y.; Zhao, D. Y. *Angew. Chem., Int. Ed.* **2001**, *40*, 2166. (c) Deng, Y. H.; Deng, C. H.; Qi, D. W.; Liu, C.; Liu, J.; Zhang, X. M.; Zhao, D. Y. *Adv. Mater.* **2009**, *21*, 1377.

(4) van Bokhoven, J. A.; Lamberti, C. *Coord. Chem. Rev.* **2014**, *277–278*, 275.

(5) Cheetham, A. K.; Férey, G.; Loiseau, T. *Angew. Chem., Int. Ed.* **1999**, *38*, 3268.

(6) (a) Goldfarb, D.; Bernardo, M.; Strohmaier, K. G.; Vaughan, D. E. W.; Thomann, H. *J. Am. Chem. Soc.* **1994**, *116*, 6344. (b) Yu, J. Q.; Feng, Z. C.; Xu, L.; Li, M. J.; Xin, Q.; Liu, Z. M.; Li, C. *Chem. Mater.* **2001**, *13*, 994. (c) Cheng, Y. T.; Jae, J.; Shi, J.; Fan, W.; Huber, G. W. *Angew. Chem., Int. Ed.* **2012**, *51*, 1387. (d) Lobo, R. F.; Davis, M. E. *J. Am. Chem. Soc.* **1995**, *117*, 3766.

(7) Eddaoudi, M.; Sava, D. F.; Eubank, J. F.; Adil, K.; Guillerm, V. *Chem. Soc. Rev.* **2015**, *44*, 228.

(8) Barrer, R. M. *J. Chem. Soc.* **1948**, 127.

(9) (a) Sendor, D.; Kynast, U. *Adv. Mater.* **2002**, *14*, 1570. (b) Wu, Y. J.; Wang, J.; Liu, P.; Zhang, W.; Gu, J.; Wang, X. J. *J. Am. Chem. Soc.* **2010**, *132*, 17989.

(10) (a) Wang, R. Y.; Zheng, Z. P.; Jin, T. Z.; Staples, R. J. *Angew. Chem., Int. Ed.* **1999**, *38*, 1813. (b) Roesky, P. W.; Canseco-Melchor, G.; Zulys, A. *Chem. Commun.* **2004**, 738. (c) Monteiro, B.; Coutinho, J. T.; Pereira, C. C. L.; Pereira, L. C. J.; Marçalo, J.; Almeida, M.; Baldoví, J. J.; Coronado, E.; Gaita-Ariño, A. *Inorg. Chem.* **2015**, *54*, 1949. (d) Messerle, L.; Nolting, D.; Bolinger, L.; Stolpen, A. H.; Mullan, B. F.; Swenson, D.; Madsen, M. *Acad. Radiol.* **2005**, *12*, S46.

(11) Kong, X. J.; Wu, Y. L.; Long, L. S.; Zheng, L. S.; Zheng, Z. P. *J. Am. Chem. Soc.* **2009**, *131*, 6918.

(12) (a) Park, K. S.; Ni, Z.; Côté, A. P.; Choi, J. Y.; Huang, R. D.; Uribe-Romo, F. J.; Chae, H. K.; O'Keeffe, M.; Yaghi, O. M. *Proc. Natl. Acad. Sci. U. S. A.* **2006**, *103*, 10186. (b) Banerjee, R. A.; Phan, A.; Wang, B.; Knobler, C.; Furukawa, H.; O'Keeffe, M.; Yaghi, O. M. *Science* **2008**, *319*, 939.

(13) Evangelisti, M.; Roubeau, O.; Palacios, E.; Camón, A.; Hooper, T. N.; Brechin, E. K.; Alonso, J. J. *Angew. Chem., Int. Ed.* **2011**, *50*, 6606.

(14) Peng, J. B.; Zhang, Q. C.; Kong, X. J.; Zheng, Y. Z.; Ren, Y. P.; Long, L. S.; Huang, R. B.; Zheng, L. S.; Zheng, Z. P. *J. Am. Chem. Soc.* **2012**, *134*, 3314.

(15) (a) Liu, J. L.; Chen, Y. C.; Guo, F. S.; Tong, M. L. *Coord. Chem. Rev.* **2014**, *281*, 26. (b) Yang, Y.; Zhang, Q. C.; Pan, Y. Y.; Long, L. S.; Zheng, L. S. *Chem. Commun.* **2015**, *51*, 7317. (c) Chen, Y. C.; Prokleška, J.; Xu, W. J.; Liu, J. L.; Liu, J.; Zhang, W. X.; Jia, J. H.; Vladimír Sechovský, V.; Tong, M. L. J. *Mater. Chem. C* **2015**, *3*, 12206.

(16) Shi, P. F.; Zheng, Y. Z.; Zhao, X. Q.; Xiong, G.; Zhao, B.; Wan, F. F.; Cheng, P. *Chem. - Eur. J.* **2012**, *18*, 15086.

(17) (a) Gao, W. Y.; Chen, Y.; Niu, Y. H.; Williams, K.; Cash, L.; Perez, P. J.; Wojtas, L.; Cai, J. F.; Chen, Y. S.; Ma, S. Q. *Angew. Chem., Int. Ed.* **2014**, *53*, 2615. (b) Omae, I. *Coord. Chem. Rev.* **2012**, *256*, 1384.

(18) (a) Beyzavi, M. H.; Klet, R. C.; Tussupbayev, S.; Borycz, J.; Vermeulen, N. A.; Cramer, C. J.; Stoddart, J. F.; Hupp, J. T.; Farha, O. K. *J. Am. Chem. Soc.* **2014**, *136*, 15861. (b) Sakakura, T.; Choi, J. C.; Yasuda, H. *Chem. Rev.* **2007**, *107*, 2365.

(19) (a) Ulusoy, M.; Çetinkaya, E.; Çetinkaya, B. *Appl. Organomet. Chem.* **2009**, *23*, 68. (b) Kilic, A.; Palali, A. A.; Durgun, M.; Tasci, Z.; Ulusoy, M. *Spectrochim. Acta, Part A* **2013**, *113*, 432.

(20) Anthofer, M. H.; Wilhelm, M. E.; Cokoja, M.; Drees, M.; Herrmann, W. A.; Kühn, F. E. *ChemCatChem* **2015**, *7*, 94.

DOI: 10.1021/jacs.5b10000
J. Am. Chem. Soc. 2015, 137, 15988–15991